JOURNAL OF CHEMICAL & ENGINEERING DATA

ARTICLE

pubs.acs.org/jced

Isothermal Vapor−Liquid Equilibrium Data for the Perfluorobutane (R610) + Ethane System at Temperatures from (263 to 353) K

Elise El Ahmar,[†] Alain Valtz,[†] Paramespri Naidoo,[‡] Christophe Coquelet,[†,‡] and Deresh Ramjugernath[*,‡]

[†]MINES ParisTech, CEP/TEP - Centre Energétique et Procédés, Rue Saint Honoré, 77305 Fontainebleau, France

[‡]Thermodynamics Research Unit, School of Chemical Engineering, University of KwaZulu-Natal, Howard College Campus, Durban, 4041, South Africa

ABSTRACT: Isothermal vapor−liquid equilibrium data for the perfluorobutane (R610) + ethane system, which were measured at seven isotherms ranging from (263.14 to 353.14) K, with pressure ranging from (0.2 to 4.6) MPa, are presented. The vapor pressure of R610 was also measured. The measurements were performed using a "static-analytic" apparatus, equipped with two pneumatic ROLSI capillary samplers, with phase analysis via gas chromatography. The measured data are correlated, and parameters are presented for two models, viz., the Peng−Robinson equation of state with the Mathias−Copeman alpha function and the Wong−Sandler mixing rules incorporating the NRTL model and the predictive Soave−Redlich−Kwong model.

INTRODUCTION

The Thermodynamics Research Unit at the University of KwaZulu-Natal, in collaboration with CEP/TEP at Mines-Paristech and some Industry partners, have initiated research into the use of fluorochemicals as potential enhancing agents in separation processes. As part of the study, vapor−liquid equilibrium data have been measured for perfluorocarbons (PFCs) with common refinery gases.

Fluorochemicals have attracted great interest from both industry and academia because they possess remarkable properties which make them suitable for applications in a number of different areas. They are used as refrigerants, fire extinguishing agents, dielectric media, solvents, and foam blowing agents, to name just a few applications.[1] The perfluorocarbons in particular show immiscibility with many common organic solvents and have high ability to dissolve gases.[2] The purpose of our large study is to investigate the absorption capabilities of perfluorocarbons with respect to common petroleum refinery gases, and as a result vapor−liquid equilibrium measurements were undertaken for ethane with perfluorobutane (R610).

Measurements of binary vapor−liquid equilibrium (VLE) for systems containing R610 have been previously undertaken by Simons et al.[3] and Gilmour et al.[4] with butane. Having undertaken an extensive literature review of the open literature, there appears to be no available vapor−liquid equilibrium data for the binary system ethane + R610.

The vapor pressure of R610 is measured. Isothermal measurements of $p-T-x-y$ data for the system were undertaken at seven isotherms. The measured data were correlated with the Peng−Robinson (PR) and the predictive Soave−Redlich−Kwong (PSRK) equations of state (EoS). Relative volatility curves, as well as the critical point loci, have been calculated for the system and are presented in the manuscript.

EXPERIMENTAL SECTION

Materials. Ethane [C_2H_6, CAS number: 74-84-0] was supplied by Messer (France) with a certified volume purity greater than 0.9995. Perfluorobutane [C_4F_{10}, CAS number: 355-25-9] was supplied by Necsa (South Africa Nuclear Energy Corporation) with a certified volume purity greater than 0.98. Both chemicals were used without any further purification, as GC analysis of the chemicals did not indicate any significant impurities. Table 1 lists the critical properties and acentric factors for the chemicals.

Experimental Apparatus. The apparatus that was used in the measurements is based on the "static-analytic" method and has been previously described by Laugier and Richon[5] and Valtz et al.[6] Temperature regulation of the equilibrium cell was via immersion in a liquid bath. The cell consists of a sapphire tube which is held between two stainless-steel flanges. Each flange contains valves and fittings for loading and venting of the cell, as well as for temperature and pressure measurements.

Internal cell pressures are measured using two pressure transducers (model: PTX 611, Druck, U.S.A.). The temperatures of the pressure transducers were regulated by means of a PID controller (model 6100, WEST, U.S.A.) and were connected to an HP data acquisition unit (HP34970A, Agilent, U.S.A.). The calibration for pressure was performed against a dead weight pressure balance (Desgranges & Huot 5202S, France). Calculated uncertainties in the pressure measurement are estimated to be within ± 0.2 kPa and ± 0.6 kPa for the low and high pressure range transducers, respectively.

Temperature measurement was via two platinum resistance thermometer probes (Pt-100 Ω, Actifa, France) which are situated within each flange, i.e., the top and bottom flange. The temperature probes were calibrated against a standard probe (25 Ohms, TINSLEY, U.K.) which was certified by the Laboratoire National d'Essai. As with pressure, logging of the temperature was also via computer interfacing to an HP data acquisition unit. Uncertainties in the temperature measurement are estimated to be within ± 0.02 K for both probes.

Received: September 16, 2010
Accepted: March 8, 2011
Published: April 11, 2011

A gas chromatograph (model: PR-2100, Perichom, France) equipped with a thermal conductivity detector (TCD) was used to analyze the equilibrium phase compositions. The column used in the gas chromatograph was supplied by Resteck, France (5 % Krytox/Carboblack B 60/80 mesh). Calibration of the detector was by repeated injection of known amounts of each pure component into the injector of the gas chromatograph using a gastight syringe. The estimated uncertainties in the equilibrium phase composition are less than 0.008 for both the vapor and liquid mole fractions.

For each equilibrium condition, at least five samples of both the vapor and liquid phases are withdrawn using the ROLSI pneumatic samplers (Mines Paristech, France) and analyzed to check for repeatability of measurements.

Experimental Procedure. The experimental procedure for all measurements consisted of the following steps: evacuation of the equilibrium cell using a vacuum pump; introduction into the cell of given quantity (approximately 5 cm^3) of the compound having the lowest vapor pressure (C_4F_{10}); setting of thermostat temperature; and introduction of a small quantity of C_2H_6. It was ensured that sufficient time was allowed for the system to reach thermodynamic equilibrium (temperature and pressure stabilization). Once it was deemed that the system was at equilibrium, sampling and analysis of liquid and vapor phases was initiated. To check for repeatability, which must be better than ± 0.001, several samples are successively withdrawn and analyzed. A new equilibrium is then produced by addition of C_2H_6. This procedure is continued until the whole composition range is covered. Once the determination of one isotherm is completed, the cell is emptied and the procedure repeated for a new isotherm. More detail on the experimental procedure is available in previous papers by Laugier and Richon[5] and Valtz et al.[6]

Table 1. Critical Parameters and Acentric Factor[7]

compound	T_c/K	P_c/MPa	ω
C_4F_{10}	385.84	2.289	0.287
C_2H_6	305.39	4.883	0.098

Table 2. Mathias−Copeman Coefficients for the PR and SRK EoS

PR EoS			SRK EoS		
coefficients	C_4F_{10}[a]	C_2H_6[13]	coefficients	C_4F_{10}[a]	C_2H_6[13]
c_1	0.935	0.531	c_1	1.120	0.675
c_2	−0.485	−0.061	c_2	−0.978	−0.308
c_3	2.100	0.214	c_3	3.209	0.462

[a] Regressed from experimental data.

MODELING

The critical parameters (temperatures (T_C) and pressures (P_C)) and acentric factors (ω) for each of the two pure components are provided in Table 1.[7]

The experimental VLE data were correlated using in-house software developed at CEP/TEP. The data were correlated using the Peng−Robinson (PR) EoS[8] incorporating the Mathias−Copeman alpha function,[9] with the Wong−Sandler[10] (WS) mixing rule utilizing the NRTL[11] activity coefficient model. This combination of model has been used previously[12] for fluorochemical + alkane systems, and modeling has been very satisfactory.

The Mathias−Copeman alpha function coefficients for both components are listed in Table 2.[13]

The predictive Soave−Redlich−Kwong (PSRK) EoS[14] was also used to calculate the VLE data for the system. This was undertaken to assess the accuracy of predictive methods.

RESULTS

The experimental vapor pressure data for C_4F_{10} (Table 3) were fitted to the PR and SRK EoS to obtain the correlated Mathias−Copeman alpha function parameters, which are listed in Table 2. The experimental VLE data are presented in Table 4 for all seven isotherms, i.e., (263.14, 283.19, 303.20, 308.20, 323.19, 338.20, and 353.14) K. The correlated parameters for the

Table 3. Experimental and Calculated Vapor Pressure for C_4F_{10} ($\Delta P = P_{exp} - P_{cal}$)[a]

		PR	SRK			PR	SRK
T/K	P_{exp}/MPa	ΔP/MPa	ΔP/MPa	T/K	P_{exp}/MPa	ΔP/MPa	ΔP/MPa
263.15	0.0727	0.0002	0.0002	303.13	0.3117	−0.0004	−0.0004
268.12	0.0896	0.0001	0.0001	307.90	0.3610	0.0004	0.0004
268.13	0.0896	0.0000	0.0000	308.21	0.3643	0.0003	0.0004
273.09	0.1094	−0.0001	−0.0001	312.88	0.4178	0.0006	0.0006
278.00	0.1324	0.00005	0.00004	317.88	0.4812	0.0007	0.0007
278.03	0.1324	−0.0001	−0.0001	322.89	0.5517	0.0006	0.0007
278.03	0.1323	−0.0002	−0.0002	323.22	0.5564	0.0004	0.0005
278.03	0.1323	−0.0002	−0.0002	327.88	0.6295	0.0007	0.0007
278.03	0.1323	−0.0002	−0.0002	332.91	0.7161	0.0008	0.0008
278.06	0.1326	0.0000	−0.0001	337.93	0.8110	0.0007	0.0006
282.99	0.1590	−0.0002	−0.0002	338.22	0.8167	0.0006	0.0005
287.91	0.1893	−0.0003	−0.0003	342.91	0.9130	−0.0009	−0.0010
292.97	0.2254	0.0001	0.0001	347.93	1.0258	−0.0023	−0.0025
297.95	0.2653	0.0002	0.0002	352.92	1.1492	−0.0031	−0.0033
302.90	0.3102	0.0003	0.0003	353.01	1.1516	−0.0030	−0.0032

[a] Calculated data via the PR EoS and SRK EoS, with the Mathias−Copeman α function.

Table 4. Experimental VLE Pressures and Phase Compositions for the C_2H_6 (1) + C_4F_{10} (2) System[a]

T/K = 263.14					T/K = 323.19				
P/MPa	n_x	x_1	n_y	y_1	P/MPa	n_x	x_1	n_y	y_1
0.1940	8	0.040	6	0.625	0.8300	6	0.048	6	0.311
0.2872	6	0.074	5	0.749	1.2204	6	0.117	6	0.515
0.3808	7	0.108	5	0.812	1.6011	5	0.186	4	0.617
0.4977	6	0.156	5	0.856	1.9841	5	0.256	5	0.681
0.6972	6	0.241	5	0.899	2.3699	6	0.328	5	0.724
0.8888	5	0.335	5	0.922	2.7761	7	0.406	5	0.757
1.0904	8	0.450	5	0.938	3.1733	7	0.486	6	0.780
1.2780	5	0.578	6	0.950	3.5574	5	0.560	5	0.796
1.4334	6	0.697	5	0.960	3.9382	7	0.633	5	0.808
1.5762	5	0.812	5	0.969	4.2774	7	0.699	5	0.814
1.6739	5	0.885	5	0.977	4.5254	7	0.752	5	0.806
1.7882	6	0.959	6	0.989	4.5677	5	0.767	5	0.799
T/K = 283.19					T/K = 338.20				
P/MPa	n_x	x_1	n_y	y_1	P/MPa	n_x	x_1	n_y	y_1
0.5007	7	0.090	5	0.677	1.1194	7	0.047	6	0.243
0.8001	8	0.176	6	0.796	1.4496	6	0.100	5	0.396
1.0712	6	0.259	8	0.847	1.7847	5	0.154	5	0.491
1.3576	6	0.356	5	0.879	2.1106	7	0.206	8	0.554
1.6174	6	0.452	6	0.899	2.4219	5	0.257	5	0.599
1.8464	6	0.544	6	0.914	2.7407	5	0.308	7	0.633
2.0786	6	0.641	6	0.927	3.0628	6	0.362	5	0.658
2.3143	8	0.742	6	0.940	3.3605	9	0.414	5	0.678
2.5499	6	0.840	5	0.955	3.6666	5	0.466	4	0.687
2.6857	5	0.891	5	0.964	3.9889	5	0.524	5	0.697
2.8202	6	0.937	5	0.977	4.3166	5	0.589	5	0.692
					4.4148	5	0.617	5	0.680
T/K = 303.20					T/K = 353.14				
P/MPa	n_x	x_1	n_y	y_1	P/MPa	n_x	x_1	n_y	y_1
0.4921	6	0.037	5	0.358	1.3981	7	0.035	6	0.145
0.9194	5	0.129	5	0.646	1.6861	5	0.077	5	0.263
1.3264	7	0.221	8	0.749	1.9884	5	0.121	6	0.349
1.7536	6	0.324	5	0.805	2.2890	9	0.166	6	0.414
2.1857	5	0.432	5	0.841	2.5711	7	0.207	5	0.459
2.6225	6	0.548	5	0.867	2.8856	9	0.254	8	0.497
3.0588	5	0.664	5	0.889	3.2033	8	0.300	5	0.527
3.4982	7	0.775	5	0.910	3.4734	7	0.346	5	0.544
3.8726	6	0.858	6	0.930	3.7705	6	0.398	6	0.550
4.1131	5	0.906	6	0.946	3.8880	5	0.420	5	0.548
4.3955	6	0.955	8	0.969	4.0030	5	0.448	7	0.536
					4.0399	7	0.459	5	0.529
					4.0469	5	0.464	5	0.526

T/K = 308.20				
P/MPa	n_x	x_1	n_y	y_1
0.5166	8	0.030	5	0.287
0.9310	8	0.114	6	0.594
1.3239	7	0.197	5	0.705

Table 4. Continued

T/K = 308.20				
P/MPa	n_x	x_1	n_y	y_1
1.7291	6	0.286	5	0.768
2.1391	7	0.381	5	0.808
2.5405	7	0.475	6	0.836
2.9334	6	0.570	7	0.857
3.3395	5	0.670	5	0.873
3.6515	5	0.742	5	0.889
3.9757	5	0.809	5	0.903
4.2642	5	0.864	5	0.918
4.5017	5	0.906	5	0.931
4.5608	6	0.916	5	0.934

[a] x,y: liquid and vapor mole fraction. n_x,n_y: number of taken samples.

Peng–Robinson EoS are presented in Table 5, and the experimental and modeled VLE data are shown in Figure 1.

To quantify the fit of the model to the experimental data, the deviation, BIASU, was determined for both the liquid and vapor phase mole fractions. The deviations are defined by:

$$\mathrm{BIASU} = (100/N)\sum((U_{\mathrm{exp}} - U_{\mathrm{cal}})/U_{\mathrm{exp}}) \qquad (1)$$

where N is the number of data points, and $U = x_1$ or y_1.

This indicator, which gives information about the agreement between model and experimental results, is presented in Table 6. It is evident that the PSRK model generally does not describe the liquid phase as well as the PR model, which seems to handle both phases reasonably well. Thus, there is probably scope for improving the functional group parameters for PSRK with the experimental data presented in this work.

The relative volatility (α_{ij}) can be calculated with the following equation

$$\alpha_{ij} = \frac{K_i}{K_j} = \frac{y_i/x_i}{y_j/xj} = \frac{y_i/x_i}{(1-y_i)/(1-x_i)} \qquad (2)$$

Uncertainties on relative volatility are calculated by considering the following relations

$$\frac{\Delta z_i}{z_i} = (1-z_i)\sum_i \frac{\Delta n_i}{n_i} \qquad (3)$$

$$\frac{\Delta \alpha_{ij}}{\alpha_{ij}} = \sum_i \frac{\Delta K_i}{K_i} \qquad (4)$$

where n_i is the number of moles; and z_i is x_i or y_i, which lead to this relation

$$\frac{\Delta \alpha_{ij}}{\alpha_{ij}} = 2\sum_i \frac{\Delta n_i}{n_i} \qquad (5)$$

The relative volatilies were computed for each of the models and compared to the experimental values. Figure 2 shows the composition dependency of relative volatility for the seven isotherms measured. There was generally very good agreement between the experimental relative volatility and those calculated using the PR EoS. The PSRK EoS did not fair as well, with representation becoming increasingly worse as temperature is decreased.

Table 5. Model Parameters Regressed for the Peng−Robinson EoS for the C_2H_6 (1) + C_4F_{10} (2) System

	T/K						
parameters	263.14	283.19	303.20	308.20	323.19	338.20	353.14
τ_{12}/J·mol^{-1}	3227	3957.4	3971.5	4183	4845.6	5095.6	7961.1
τ_{21}/J·mol^{-1}	321	−48.3	−255.1	−383.6	−699.1	−910.3	−1492.9
k_{ij}	0.379	0.371	0.374	0.375	0.373	0.379	0.372

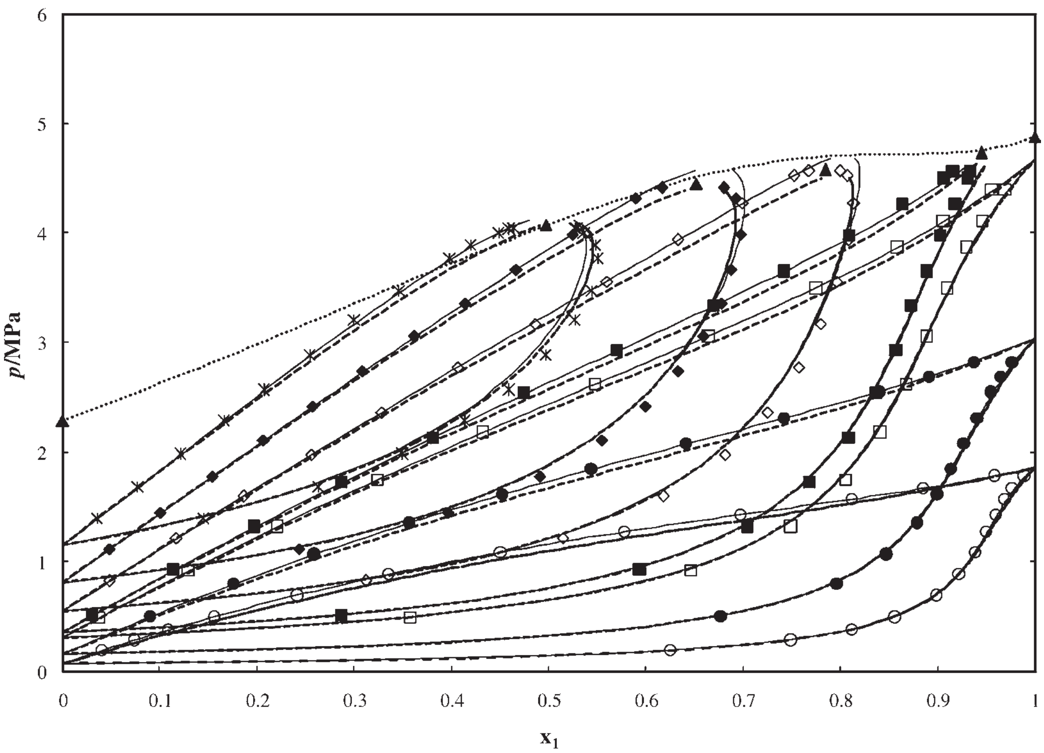

Figure 1. Phase diagrams (P−x−y) for the C_2H_6 (1) + C_4F_{10} (2) system. ○, 263.14 K; ●, 283.19 K; □, 303.20 K; ■, 308.20 K; ◇, 323.19 K; ♦, 338.20K; ∗, 353.14 K; ▲, critical point value; ····, critical locus; —, PR EoS; - - - -, PSRK model.

Table 6. Relative Deviation BIASU Obtained in Fitting Experimental VLE Data with PR EoS and PSRK Model

	PR		PSRK	
T/K	bias x (%)	bias y (%)	bias x (%)	bias y (%)
263.14	−0.01	0.15	−8.10	0.01
283.19	0.09	0.22	−3.76	0.07
303.20	−0.10	0.61	−2.17	0.58
308.20	−0.16	0.52	−2.22	0.61
323.19	−0.12	0.83	−2.38	1.68
338.20	−0.34	1.37	−2.42	2.26
353.14	−0.69	2.71	−3.57	1.77

Critical Point Determination. It is possible, by using the experimental data, to calculate the critical point (composition and pressure). The critical loci for the binary mixture and the near-critical phase behavior have been approximated by the use of extended scaling laws, as proposed by Ungerer et al.[15] In their method, the near-critical part of the pressure−composition diagram is represented by complementing the near-critical scaling law with a linear term.

$$y - x = \lambda_1(P_c - P) + \mu(P_c - P)^{\beta} \tag{6}$$

$$\frac{y + x}{2} - x_c = \lambda_2(P_c - P) \tag{7}$$

where β is a constant and P_c, x_c (critical coordinates) and λ_1, λ_2, μ (adjustable coefficients) are regressed from a set of coexistence points (P, x, y) below the critical point.

Table 7 lists the mixture critical points for the isotherms where one of the components is above its critical temperature.

Procedures to calculate critical points using EoS were initially proposed by Heidemann and Khalil[16] and Michelsen and Heidemann.[17] They assumed that the stability criterion for an isothermal variation (between an initial state and a very close new state) can be described by a minimization of the molar Helmholtz energy

$$A - A_0 - \sum_i \mu_{io}\Delta n_i \geq 0 \tag{8}$$

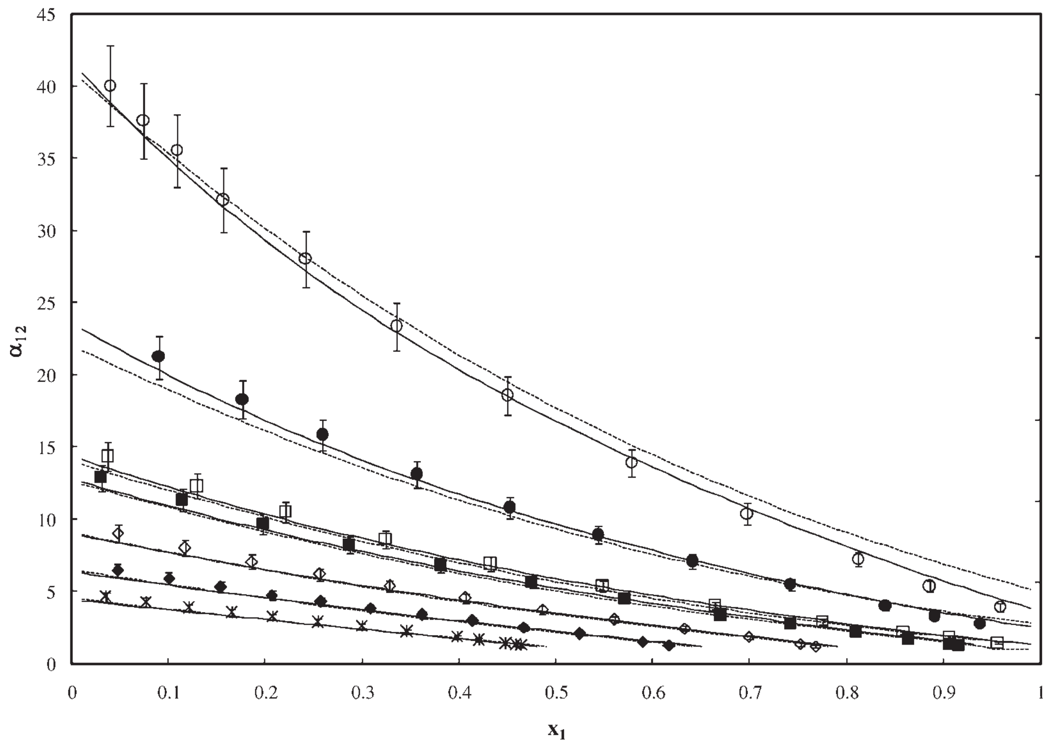

Figure 2. Plot of relative volatility (α_{12}) against mole fraction for the C_2H_6 (1) + C_4F_{10} (2) system. ○, 263.14 K; ●, 283.19 K; □, 303.20 K; ■, 308.20 K; ◇, 323.19 K; ♦, 338.20K; *, 353.14 K; —, PR EoS; - - - -, PSRK model. Error bands: ± 7 % for experimental results.

Table 7. Determination of Critical Point Using Scaling Laws and Experimental Data for the C_2H_6 (1) + C_4F_{10} (2) System

T/K	P_c/MPa	x_{1c}
308.20	4.74	0.945
323.19	4.58	0.785
338.20	4.45	0.652
353.14	4.10	0.497

where $A - A_0$ is the difference in Helmholtz free energy between the varied and the initial state; μ_{io} is chemical potentials at the initial state; and Δn_i is variation of the number of moles.

The critical point corresponds to the limit of stability. They developed an algorithm to calculate the critical point with a van der Waals type EoS, combined with the classical mixing rules. Stockfleth and Dohrn[18] improved this method by generalizing the previous algorithm. The Stockfleth and Dohrn[18] method was used in this work to calculate the critical loci using the PR EoS with Wong−Sandler mixing rules and the NRTL model. The binary parameters used in the method were those obtained by correlating the VLE data in the ethane supercritical domain. Results using the Stockfleth and Dohrn[18] method for this system are reported in Table 8, and Figure 3 shows the PT diagram for the system, with the pure component vapor pressure curves predicted with the PR EoS with Mathias−Copeman parameters.

■ DISCUSSION

The PR EoS model represents the experimental better than the PSRK model, and this is expected, as the PR model is correlative, while the PSRK model is predictive. The

Table 8. Prediction of Critical Point Using the PR EoS for the C_2H_6 (1) + C_4F_{10} (2) System

T_c/K	P_c/MPa	x_{1c}	T_c/K	P_c/MPa	x_{1c}
385.84	2.29	0.0	354.24	4.08	0.5
381.03	2.63	0.1	345.09	4.38	0.6
375.59	2.99	0.2	334.86	4.61	0.7
369.39	3.36	0.3	323.81	4.71	0.8
362.31	3.73	0.4	312.98	4.73	0.9
			305.39	4.88	1.0

representation with both models is much better at the higher temperatures of measured data. The poorest fitting of the experimental data was for the 263.14 K isotherm (see Table 6). Using the PR model, the data are well correlated except for the region close to the mixture critical point, for which there is a poor fit. Using the scaling laws with the experimental data, we have predicted the mixture critical point. Of course, this prediction is dependent on the numbers of data points available, but the estimation seems to be close to reality. We have tried to determine accuracy of the critical temperature and pressures using eqs 9 and 10 for the estimated critical point using scaling laws and the predicted ones using the PR EoS model.

$$\Delta T_c = T_c - \sum_i x_i T_{c_i} \tag{9}$$

$$\Delta P_c = P_c - \sum_i x_i P_{c_i} \tag{10}$$

Figure 4 presents the results using eqs 9 and 10. The PR EoS can be clearly seen to overpredict the critical point. Moreover, the

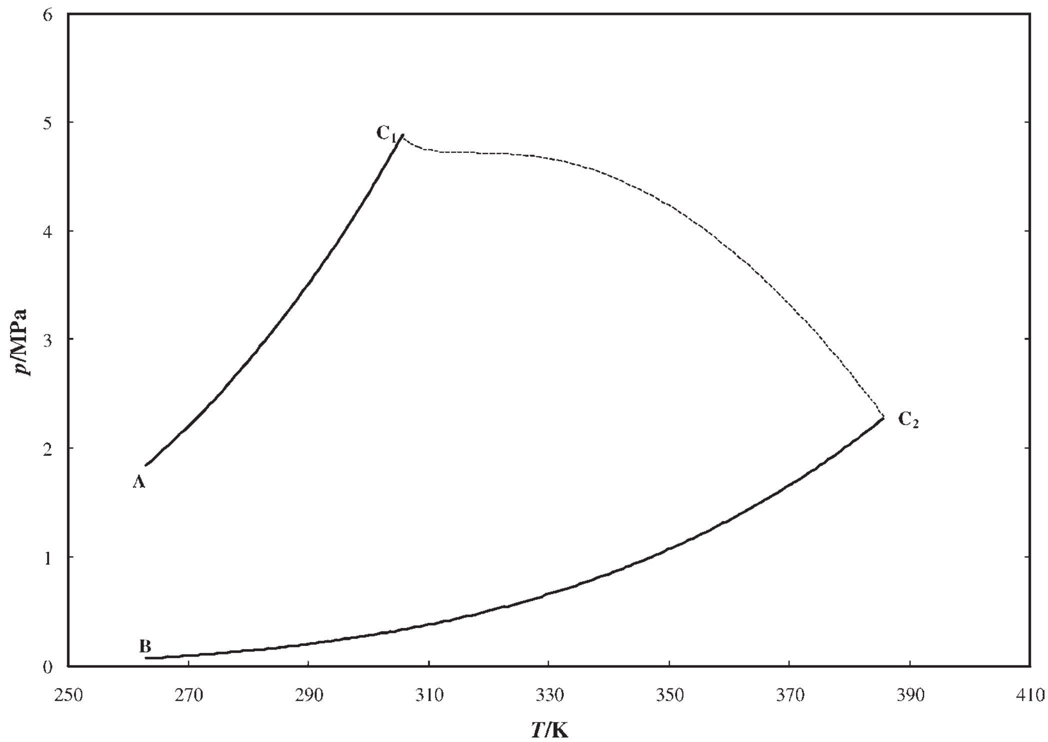

Figure 3. *PT* diagram for the C_2H_6 (1) + C_4F_{10} (2) system. Dashed line: critical loci calculated with the PR EoS. Curve A−C1 (C_2H_6 pure component vapor pressure) and Curve B−C2 (C_4F_{10} pure component vapor pressure) are calculated with the PR EoS.

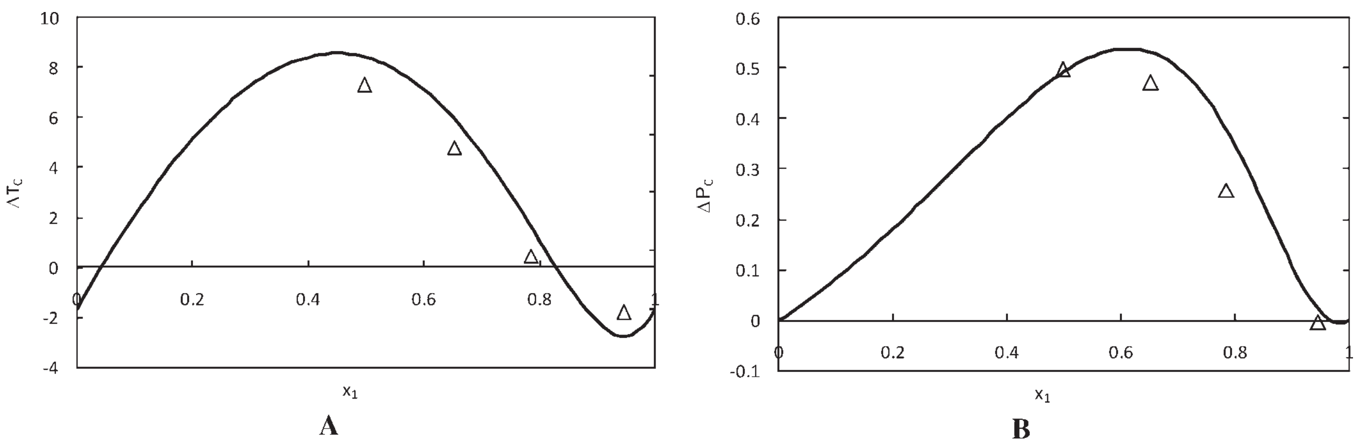

Figure 4. Evolution of ΔT_c (A) and ΔP_c (B) for the C_2H_6 (1) + C_4F_{10} (2) system as a function of C_2H_6 mole fraction. Δ, critical point value using scaling laws; solid line, PR EoS.

critical loci seem to present a "memory effect" of the shape of the subcritical isotherm for temperatures just above the C_2H_6 critical temperature. Therefore, to obtain better representations of the critical point, it would be necessary to use another model which probably would be the "crossover EoS".[19,20]

CONCLUSIONS

In this paper, VLE data for the system C_2H_6 + C_4F_{10} are presented at seven temperatures. The experimental data have not been previously reported in the open literature. The experimental setup using a "static-analytic" method is completely described, and the uncertainties concerning the apparatus calibration are also given. The experimental vapor pressures for C_4F_{10} were fitted to the PR and SRK EoS, and adjusted Mathias−Copeman function parameters were obtained and are reported. The experimental data were modeled with the PR EoS, as well as the PSRK EoS. The PR EoS with Wong−Sandler mixing rules and the NRTL Gibbs energy function are able to produce reliable correlation of the data and can be used for relative volatility and critical loci representation and prediction with reasonable accuracy.

AUTHOR INFORMATION

Corresponding Author

*E-mail: ramjuger@ukzn.ac.za. Tel.: +27 31 2603128. Fax: +27 31 2601118.

Funding Sources

This work is based upon research supported by the South African Research Chairs Initiative of the Department of Science and Technology and National Research Foundation.

■ ACKNOWLEDGMENT

Special thanks to Pelchem and NECSA who supplied the perfluorobutane.

■ REFERENCES

(1) Lindley, A. A.; McCulloch, A. Regulating to reduce emissions of fluorinated greenhouse gases. *J. Fluorine Chem.* **2005**, *126*, 1457–1462.

(2) Banks, R. E.; Tatlow, J. C. A guide to modern organofluorine chemistry. *J. Fluorine Chem.* **1986**, 33–227.

(3) Simons, J. H.; Mausteller, J. W. The properties of n-Butforane and its mixtures with n-Butane. *J. Chem. Phys.* **1952**, *20*, 1516–1519.

(4) Gilmour, J. B.; Zwicker, J. O.; Katz, J.; Scott, R. L. Fluorocarbon solutions at low temperatures. Part V. *J. Phys. Chem.* **1967**, *71*, 3259–3270.

(5) Laugier, S.; Richon, D. New apparatus to perform fast determinations of mixture vapor-liquid equilibria up to 10 MPa and 423 K. *Rev. Sci. Instrum.* **1986**, *57*, 469–472.

(6) Valtz, A.; Coquelet, C.; Baba-Ahmed, A.; Richon, D. Vapor-liquid equilibrium data for the propane + 1,1,1,2,3,3,3-heptafluoropropane (R227ea) system at temperatures from 293.16 to 353.18 K and pressures up to 3.4 MPa. *Fluid Phase Equilib.* **2002**, *202*, 29–47.

(7) *Dortmund Data Bank (DDB)*, version 2002; DDBST Software and Separation Technology GmbH: Oldenburg, Germany.

(8) Peng, D. Y.; Robinson, D. B. A new two constant equation of state. *Ind. Eng. Chem. Fundam.* **1976**, *15*, 59–64.

(9) Mathias, P. M.; Copeman, T. W. Extension of the Peng-Robinson Equation of State to Complex Mixtures: Evaluation of Various Forms of the Local Composition Concept. *Fluid Phase Equilib.* **1983**, *13*, 91–108.

(10) Wong, D. S. H.; Sandler, S. I. A Theoretically Correct Mixing Rules for Cubic Equations of State. *AIChE J.* **1992**, *38*, 671–680.

(11) Renon, H.; Prausnitz, J. M. Local Composition in Thermodynamic Excess Function for Liquid Mixtures. *AIChE J.* **1968**, *14*, 135–144.

(12) Ramjugemath, D.; Valtz, A.; Coquelet, C.; Richon, D. Isothermal vapor-liquid equilibrium data for the hexafluoroethane (R116) + propane system at temperatures from (263 to 323) K. *J. Chem. Eng. Data* **2009**, *54*, 1292–1296.

(13) Reid, R. C.; Prausnitz, J. M.; Poling, B. E. *The properties of gases and liquids*; McGraw-Hill Book Company: New York, USA, 1987.

(14) Holderbaum, T.; Gmehling, J. PSRK: A Group Contribution Equation of State Based on UNIFAC. *Fluid Phase Equilib.* **1991**, *70*, 251–265.

(15) Ungerer, P.; Tavitian, B.; Boutin, A. *Applications of molecular simulation in the oil and gas industry- Monte Carlo methods*; Edition Technip: Paris, 2005.

(16) Heidemann, R. A.; Khalil, A. M. The calculation of critical points. *AIChE J.* **1980**, *26*, 769–779.

(17) Michelsen, M. L.; Heidemann, R. A. Calculation of critical points from cubic 2 constant equations of state. *AIChE J.* **1981**, *27*, 521–523.

(18) Stockfleth, R.; Dohrn, R. An algorithm for calculating critical points in multicomponents mixtures. *Fluid Phase Equilib.* **1998**, *45*, 43–52.

(19) Kiselev, S. B. Cubic Crossover equation of state. *Fluid Phase Equilib.* **1998**, *147*, 7–23.

(20) Dicko, M.; Coquelet, C. Application of a New Crossover Treatment to a Generalized Cubic Equation of State. *Fluid Phase Equilib.* **2011**, *302*, 241–248.